A Novel Electrolyte-Responsive Membrane with Tunable Permeation Selectivity for Protein Purification

Yong-Hong Zhao, Kin-Ho Wee, and Renbi Bai*

Division of Environmental Science and Engineering, Faculty of Engineering, National University of Singapore, 9 Engineering Drive 1, Singapore 117576, Singapore

ABSTRACT A novel electrolyte-responsive membrane, RC-*g*-PSBMA, was successfully prepared from regenerated cellulose (RC) membrane through surface-initiated atom transfer radical polymerization (ATRP) of a zwitterionic monomer, sulfobetaine methacrylate (SBMA). Different degrees of polymerization for the grafted SBMA polymers (i.e., PSBMA) on the RC membrane were easily obtained by adjusting the ATRP reaction conditions. The electrolyte-responsive behavior of RC-*g*-PSBMA was first evaluated through the permeation experiments with sodium chloride (NaCl) solutions of different concentrations. It was found that the permeability of RC-*g*-PSBMA showed a clear dependence on NaCl concentration in the solutions. To further examine the potential of RC-*g*-PSBMA for protein purification, bovine serum album (BSA) was chosen as a model protein and polystyrene nanoparticles (NPs) of different sizes were used as representative impurities in the solutions. The rejection rates of BSA and NPs by RC-*g*-PSBMA were examined with the solutions containing BSA and NPs at different NaCl concentrations. The results showed that the rejection rates of BSA were at a very low level regardless of the concentration of NaCl in the solutions, indicating that the membrane allowed BSA to permeate. However, the rejection rates of NPs of different sizes by RC-*g*-PSBMA changed remarkably with the concentration of NaCl in the solutions. The study has demonstrated the possibility to separate BSA from NPs of different sizes by using the same membrane but simply altering the concentration of NaCl in the solutions. Membranes with such properties will have a great potential for protein purification as well as for many other separation applications.

KEYWORDS: electrolyte-responsive membranes • tunable permeation selectivity • ATRP • ziwitterionic polymer • protein purification

INTRODUCTION

With the rapid development of biotechnology, worldwide demand for protein therapeutics has increased rapidly in recent years (1). Because of the presence of a large number of impurities, such as pyrogens and viruses, etc., the purification of proteins is of critical importance for protein-related biopharmaceutical products and research (2). Membrane-based separation technology has been identified as a useful method for the purification of biomaterials, including proteins, because of its good efficiency, ease of implementation, and cost effectiveness (3). However, for a specific membrane, the scope of its applicability is usually limited because of the fixed pore size (4). For example, when the sizes of proteins or impurities to be separated change, a new type of membrane with another corresponding pore size has to be used in order to maintain a high efficiency in the separation performance. To extend the application prospects of membrane separation processes, it is highly desirable to develop membranes that have the capability to adjust their permeation selectivity according to the sizes of proteins and impurities to be separated.

Stimuli-responsive porous membranes that can change their permeation/separation properties have been the focus of research for the last few decades (5–7). In most studies, the stimuli-responsive membranes were prepared by surface modification of commercially available porous membranes with polymers that can expand or contract in response to external stimuli, such as pH (8–15), temperature (16–22), electric field (23, 24), ionic strength (25, 26), or light (27) of the environment. When such membranes are applied in separation processes, the permeation selectivity can be easily tuned by manipulation of the environmental and operational conditions. Hence, the feature of stimuli-responsive change in pore size and surface properties can be potentially used to develop novel protocols that are suitable for the separation of biomaterials of different sizes using just one tunable membrane.

Sulfobetaine polymers belong to a special class of zwitterionic polyelectrolytes, in which ammonium cation and sulfonic anion are located on the same monomer residue (28). It was found that the solutions of sulfobetaine polymers do not exhibit the behaviors of common polyelectrolytes (29). Because of the electrostatic attraction among the opposite charges, the molecules of sulfobetaine polymers are in a collapsed and globular conformation in an aqueous solution. The presence of inorganic salts, such as sodium chloride (NaCl), will shield the intra- and/or interchain associations of the charges, allowing the sulfobetaine polymer

* Corresponding author. E-mail: esebairb@nus.edu.sg. Phone: +65 6516 4532. Fax: +65 6774 4202.
Received for review September 28, 2009 and accepted December 11, 2009
DOI: 10.1021/am900654d

chains to adopt a more extended molecular conformation, which is called the "anti-polyelectrolyte effect" (30–33). More importantly, because of the strong capability to form a hydration layer via electrostatic interaction between zwitterions and water molecules, sulfobetaine polymers are recognized as a type of biocompatible materials with excellent anti-protein-fouling properties (34–36). Hence, there is a great prospect to use sulfobetaine polymers to functionalize conventional membranes to obtain the desired electrolyte-responsive membranes for the purification of proteins. This will, on one hand, restrain protein-fouling of membranes when proteins are separated by membrane processes and, on the other hand, achieve tunable permeation selectivity of the membranes by altering the salt concentration in the feed solutions, which makes it possible to efficiently separate proteins from impurities of different sizes without the need to change the membranes.

Because of the presence of hydroxyl groups, regenerated cellulose (RC) membrane provides a versatile platform for further functionalization. Husson and coworkers have reported the modification of RC membranes with various monomers through the surface-initiated atom transfer radical polymerization (ATRP) method (37–40). In the present work, we prepared a novel electrolyte-responsive membrane by grafting poly(sulfobetaine methacrylate) (PSBMA) to the RC membrane via ATRP. ATRP was used because it is a controllable chain growth technique that provides us the possibility to control the chain length of the grafted polymers, which, in turn, allows the control of the permeation/separation selectivity of the prepared membrane. By adjusting the ATRP reaction conditions, we grafted PSBMA polymers with different degrees of polymerization to the RC membrane. The prepared membrane, denoted as RC-*g*-PSBMA, was examined for their permeation responses to the concentrations of NaCl in solutions. Then, solutions containing bovine serum album (BSA) or polystyrene nanoparticles (NPs) of different sizes were filtered through RC-*g*-PSBMA. By examining the rejection behavior of RC-*g*-PSBMA for BSA and NPs at different NaCl concentrations in the solutions, the potential of the prepared electrolyte-responsive membrane to be used for protein purification has been addressed.

EXPERIMENTAL SECTION

Materials. RC porous membranes with an average pore size of 0.2 μm were purchased from Whatman. The RC membranes were dried at 40 °C and cooled down to room temperature (22−23 °C) in a vacuum oven until constant weights before use. 2-(*N*-3-Sulfopropyl-*N*,*N*-dimethyl ammonium)ethyl methacrylate (SBMA) (97%), 2.2′-bipyridyl (Bpy) (≥ 99%), CuBr (98%), $CuBr_2$ (97%), 2-bromoisobutyryl bromide (98%), bovine serum albumin (BSA) (molecular weight: ~66 kDa), cetylpyridinium chloride (CPC), cetyl-triammonium bromide (CTAB), 2,2′-azobis(2-methylpropionamidine) dihydrochloride (V-50, 97%) and styrene (99%) were purchased from Sigma-Aldrich and used as received. Tetrahydrofuran (THF) from Merck was dried by sodium before use. Triethylamine (TEA) from Aldrich was purified by distillation and stored in 4 Å molecular sieves. Methanol, NaCl, and NaOH were analytical grade and used without further purification. Deionized (DI) water (18 MΩ) purified with a Milli-Q system from Millipore was used in all syntheses and analyses as needed in the study. The phosphate-buffered saline solution

Scheme 1. Schematic Representation for the Surface-Initiated ATRP of SBMA from RC Membrane

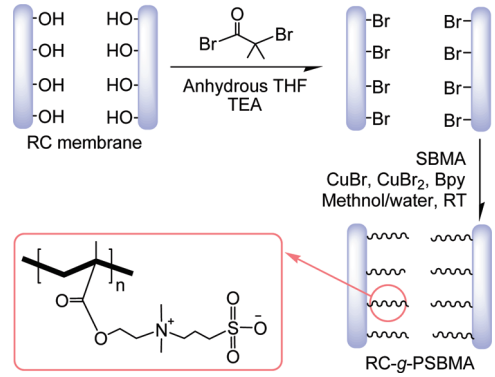

(PBS, pH 7.0, 0.02 M ionic strength) was prepared by the addition of the prepackaged buffer salts (Aldrich) into DI water.

Surface-Initiated ATRP of SBMA. The entire process for the surface-initiated ATRP of SBMA from the surface of the RC membrane is shown in Scheme 1. Firstly, under nitrogen protection, three pieces of the RC membranes (d=47 mm and about 0.066 g for each piece) were reacted with 2-bromoisobutyryl bromide (2 mL) at 0 °C in the presence of TEA with anhydrous THF as the solvent. The reaction was conducted at a significant excess of the initiator as compared to the amount of −OH in the RC membranes. After the reaction, the membrane (denoted as RC-Br) was washed sequentially with methanol−DI water−methanol. Then, CuBr (1 mmol), $CuBr_2$ (0 or 0.25 mmol, respectively), and three pieces of RC-Br were placed into a three-necked flask under nitrogen protection. SBMA (7.5 mmol) and Bpy (2 mmol) were first dissolved in a 25 mL DI water/methanol (1/1, v/v) mixture and the solution was then transferred into the flask after being purged with nitrogen for 30 min. The reaction mixture in the flask was stirred at room temperature for a predetermined time and the reaction was then terminated by exposing the mixture to air. After being thoroughly washed with methanol and DI water, the membranes were dried under vacuum at 40 °C for 24 h to constant weights before their characterization analysis. The membrane prepared from this process is referred to as RC-*g*-PSBMA.

Characterization of Membranes. ***Surface Chemical Compositions.*** The surface chemical compositions of the membranes were characterized by attenuated total reflectance Fourier transform infrared spectroscopy (FTIR/ATR) and X-ray photoelectron spectroscopy (XPS). FTIR/ATR measurements were carried out on a Shimadzu H8400 (Japan) instrument equipped with an ATR cell (KRS-5 crystal, 45°). Sixteen scans were performed at a resolution of 4 cm^{-1} for each spectrum. XPS analyses were conducted on an AXIS HIS spectrometer (Kratos Analytical Ltd., U.K.) with an Al Kα X-ray source (1486.71 eV of photons). The X-ray source was run at 250 W with an electron takeoff angle of 45° relative to the sample surface. The pressure in the analysis chamber was maintained at about 5×10^{-7} Pa during each measurement. The survey spectra (from 0 to1200 eV) and core-level spectra with much higher resolutions were both collected. In the analyses, all binding energies were referenced to the neutral C 1s peak at 284.6 eV to compensate for possible surface charging effects. The software package XPSpeak 4.1 was used to fit the XPS spectra peaks.

Surface Morphology. The top surface morphologies of the membranes were observed with a field emission scanning electron microscope (FESEM, JEOL JEM-6700) under standard high-vacuum conditions. Samples were dried under vacuum and coated with platinum by a vacuum electric sputter coater

(JEOL JFC-1300) before being mounted onto the sample stud for the SEM observation.

Filtration Tests. The performance of the electrolyte-responsive membrane was assessed with a dead-end filtration system, including an air gas cylinder, a pressure controller (Alicat Scientific PCD, USA), a clear plastic reservoir, and a Advantec Stirred Cell (effective filtration area: 11.9 cm^2, Advantec UHP-43, Japan) coupled with a magnetic stirrer. Before the filtration tests, all the sample membranes were filtered with DI water until their fluxes became constant.

Fluxes of NaCl Solutions. NaCl solutions with concentrations at 0, 0.02, 0.04, 0.06, 0.08, and 0.1 M were used in the flux measurements. A sample membrane mounted on the stirred cell was soaked in the same NaCl solution to be filtered for 30 min before the flux measurement started. The fluxes were calculated from the collected weights of the solution permeated through the membrane for per unit time per unit area under a specific trans-membrane pressure (0.02 MPa).

Rejection of BSA. BSA solutions with a concentration of 1.0 g/L were prepared with the PBS solution and were adjusted to different NaCl concentrations. A 1 L amount of each of the BSA solutions was filtered through the membrane being tested after the membrane was soaked in the same solution for 30 min. The rejection rate of BSA was calculated from the ratio of the BSA concentration in the permeate solution to that in the feed. BSA concentrations in the solutions were determined from the absorbance intensity at 280 nm with a UV−vis spectrophotometer (Agilent 8453). (BSA concentration in the permeate solution was the average of the permeate solution collected from the 1 L feed).

Rejection of NPs. NPs of two different sizes were synthesized according to the classical methods of emulsion polymerization suggested by Lovell et al. (41). The detailed synthesis procedure is provided in the supporting information. NP stock solutions were mixed with DI water or NaCl solution to obtain 0.1 g/L suspensions. For the NP suspensions with NaCl solution, an additional cationic surfactant, cetyl-triammonium bromide (CTAB), was added to enhance the colloidal stability of the NP suspensions in against electrolyte-induced coagulation. Typically, 0.067 g of CTAB was added for every 100 mL of the NP suspension prepared, which would give a surfactant concentration that is two times of its critical micelle concentration ($CMC_{CTAB} \approx 0.92$ mM). A 200 mL amount of a NP suspension was filtered through the membrane being tested after the membrane was soaked in the same suspension for filtration for 30 min. The rejection rates of NPs were similarly determined as for those of BSA. The concentrations of NPs in the feed and permeate solutions were measured from the absorbance intensity at 254 nm with the UV−vis spectrophotometer (NP concentration in the permeate solution was the average of the permeate solution collected from the 200 mL feed).

Anti-Protein-Fouling Evaluation. In this part of the study, the flux of PBS solution was measured in the first 1 h after the membrane was soaked in the solution for 30 min. Then, a solution containing 1g of BSA per liter prepared from the PBS solution was filtered through the membrane for 3 h and the corresponding permeate flux was recorded against the time. After that, the membrane was washed by shaking in a 0.1 M NaOH solution for 1 h and rinsed in DI water for another 1 h. Then, the flux for PBS solution was measured again for 1 h after the membrane was immersed in the solution for 30 min.

RESULTS AND DISCUSSION

Surface Chemical Features. The characterestic chemical compositions of RC, RC-Br and RC-*g*-PSBMA from the FTIR/ATR analysis are shown in Figure 1. Two characteristic peaks were observed in the spectrum of the RC membrane (Figure 1a). The sharp peak around 1034 cm^{-1} is attributed to the C−O stretching vibrations in −C−OH and C−O−C groups, and the broad absorption band centering at 3384 cm^{-1} is the typical stretching vibrations of hydroxyl groups in hydrogen-bond state. After the imobilization of the ATRP initiator, the strength of the peak at 3384 cm^{-1} decreased significantly (see Figure 1b), indicating the conversion of the hydroxyl groups to corresponding esters, which was consistent with the increase of the C═O peak at 1725 cm^{-1}. In the spectrum of RC-*g*-PSBMA (see Figure 1c), the characteristic new peak at 1165 cm^{-1} for the stretching vibration of the sulfonate groups and the increased strength of the C═O peak at 1725 cm^{-1} confirm the successful polymerization of SBMA on RC-Br in the ATRP process. The broad absorption band at 3408 cm^{-1} (Figure 1c) may be ascribed to the H_2O molecules adsorbed on the PSBMA chains, since PSBMA is extremely hydrophilic (34) and it is difficult to remove the moisture completely from the sample during the FTIR/ATR measurements. Therefore, the FTIR results in Figure 1 support the reaction processes given in Scheme 1.

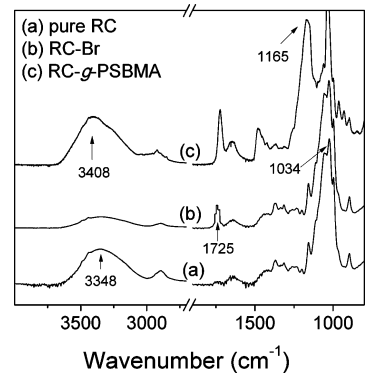

FIGURE 1. FTIR/ATR spectra of (a) RC, (b) RC-Br and (c) RC-*g*-PSBMA (ATRP conditions: [CuBr]/[$CuBr_2$]/[Bpy]/[SBMA] = 1/0.25/2/7.5; water/methanol = 1/1; ATRP reaction time = 24 h).

XPS analysis was also used to characterize the chemical compositions of the membrane surfaces qualitatively as well as quantitatively. Figure 2 shows the XPS survey spectra of RC, RC-Br, and RC-*g*-PSBMA. Because there are two major elements (i.e., C and O) besides hydrogen in the chemical structure of RC, two emissions at 284.6 and 532.0 eV, assigned to the binding energy of C 1s and O 1s, respectively, were indeed observed in the XPS spectrum of RC (see Figure 2a). After the imobilization of the ATRP initiator, the characteristic peak of Br 3s (255.2 eV), Br 3p (182.2 eV), and Br 3d (69.0 eV) appeared in the XPS spectrum of RC-Br [see Figure 2(b)]. In the spectrum of RC-*g*-PSBMA, the new emission peaks at 165.8 eV (S 2p) and 400.8 eV (N 1s) confirmed the successful polymerization of SBMA initiated from RC-Br in the ATRP process. To provide more detailed information about the change of the chemical compositions on the membrane surfaces in the preparation process, further high-resolution O 1s spectra, as shown in Figure 3, were also collected. For the RC membrane surface (Figure 3a), the intensity profile of O 1s core-level spectrum could be fitted into two peaks at 532.6 eV and 533.06 eV, corresponding to the groups of *O*−H and C−*O*−C, respectively. When the hydroxyl groups in RC were esterified by the ARTP

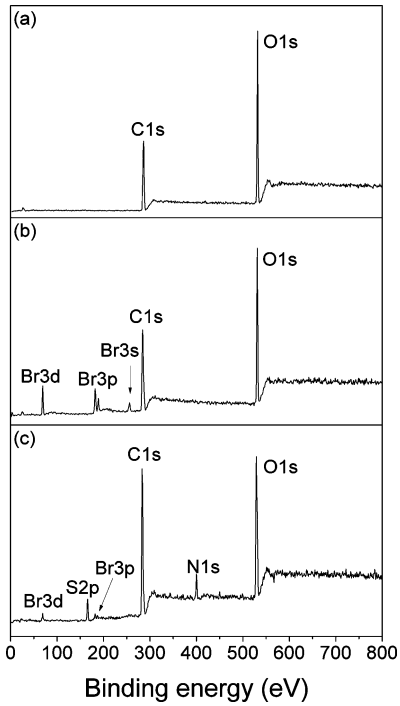

FIGURE 2. XPS survey spectra of (a) RC, (b) RC-Br and (c) RC-*g*-PSBMA (ATRP conditions: [CuBr]/[$CuBr_2$]/[Bpy]/[SBMA] = 1/0.25/2/7.5; water/methanol = 1/1; ATRP reaction time = 24 h).

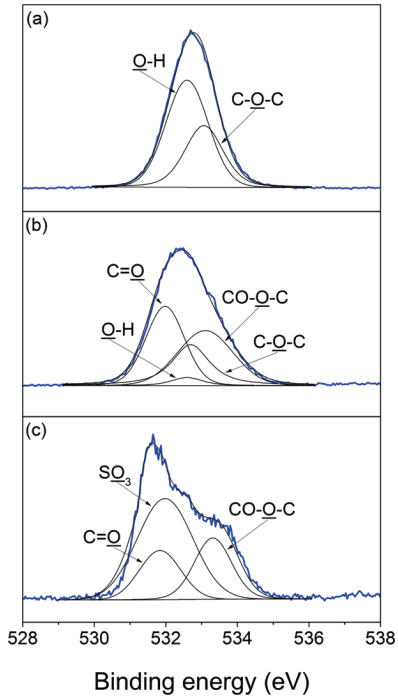

FIGURE 3. O 1s core-level XPS spectra of (a) RC, (b) RC-Br, and (c) RC-*g*-PSBMA (ATRP conditions: [CuBr]/[$CuBr_2$]/[Bpy]/[SBMA] = 1/0.25/2/7.5; water/methanol = 1/1; ATRP reaction time = 24 h).

initiator, the relative intensity of the *O*—H peak at 532.6 eV decreased almost completely(Figure 3b), and new peaks at 533.3 eV ascribed to CO—*O*—C groups and at 531.8 eV for C═*O* groups appeared. After the surface initiated ATRP of SBMA, a new and strong peak at 532.0 eV attributed to the oxygen in the sulfonate groups was clearly observed in the O 1s core-level spectrum of the RC-*g*-PSBMA surface (Figure 3c). The XPS results in Figures 2 and 3 are hence consistent with the FTIR/ATR results in Figure 1 and confirm the successful grafting of PSBMA on the RC membrane.

Table 1. Elemental Compositions (mol %) of the RC-*g*-PSBMA Membrane Surfaces under Different ATRP Reaction Conditions Obtained from XPS Analysis

	ATRP time (h)							
	[CuBr]/[$CuBr_2$] 1/0				[CuBr]/[$CuBr_2$] 1/0.25			
element (mol %)	6	12	18	24	6	12	18	24
C	63.80	63.23	62.89	62.80	63.81	62.98	63.07	62.06
N	3.94	4.33	4.64	4.59	3.46	4.55	4.91	5.32
O	28.31	28.03	27.90	27.98	29.17	27.98	27.31	27.41
S	3.75	4.20	4.35	4.42	3.25	4.37	4.63	5.15
Br	0.20	0.21	0.22	0.21	0.31	0.12	0.08	0.06

Extent of Polymerization. In an ATRP process, the deactivator is the higher oxidation state metal complex formed after atom transfer and it plays a vital role in ATRP in reducing the polymerization rate and the polydispersity of the final polymer (42). To achieve satisfactory control in ATRP, a high concentration of deactivator, such as Cu(II), is necessary (43). In a typical ATRP process, a few percent of chains terminate at the very beginning of the reaction and spontaneously form deactivating Cu(II) species, which are usually sufficient for a controlled radical polymerization to commence (43). However, in surface-initiated ATRP, the concentration of surface initiator with respect to reaction volume is usually extremely low and the number of deactivators generated in the beginning of the polymerization is often not sufficient for good control. To overcome this problem, a widely used remedy is to add sacrificial initiator to the system. The termination of free chains in the solution then generates a sufficient amount of deactivator (44, 45). Unfortunately, adding sacrificial initiator always results in excessive polymerization of monomer in the solution and often makes the reaction system inhomogeneous. An alternative is to add Cu(II) complex at the beginning of polymerization. In this work, the effect of the concentration of Cu(II) complex on the controllability of the ATRP process was investigated. Table 1 summarizes the elemental compositions, measured from XPS analysis, of the RC-*g*-PSBMA membrane surfaces under various ATRP conditions. Although all the initiator molecules on the membrane surface may not function exactly the same, we estimated the degree of polymerization (DP) of PSBMA by assuming the PSBMA chains would grow from each initiator uniformly so as to provide a basis for comparison of DP under different ATRP conditions. On the basis of the results in Table 1, the approximate DP of PSBMA on the membrane surfaces are calculated and shown in Figure 4 (the estimation method is given in the caption of Figure 4). It can be found that the growth of the PSBMA chains greatly slowed down and the DP appeared to approach a maximum after 6 h of the reaction when no Cu(II) complex was added in the catalyst system. As a result, the achieved DP was at a relatively low level. With 25% $CuBr_2$ (relative to CuBr) added to the reaction system, the initial rate of polymerization was

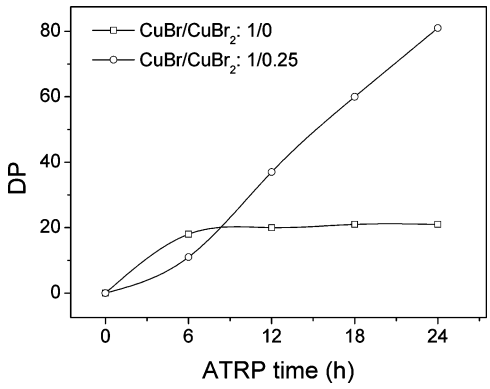

FIGURE 4. Dependence of the estimated DP of PSBMA chains on the membrane surface upon the ATRP conditions. ([CuBr]/[$CuBr_2$]/[Bpy]/[SBMA] = 1/0/2/7.5 (□) and 1/0.25/2/7.5 (○); water/methanol=1/1). Calculation method: DP = ([N] + [S])/(2[Br]), where [N], [S], and [Br] are the mole percentage of N, S, and Br given in Table 1, respectively. For the convenience of calculation, we assumed that the PSBMA chains grew from every initiator equally.

slightly lower than that in the absence of Cu(II) complex in the first 6 h, but the DP increased continuously over the whole course of the polymerization (24 h). As suggested by Matyjaszewski et al. (46), the addition of a small amount of Cu(II) halides at the beginning of the polymerization can reduce the proportion of terminated chains and help establish the atom transfer equilibrium. The increase in Cu(II) halides shifts the equilibrium toward the dormant species, leading to a slower polymerization rate, and subsequently, a more controllable polymerization process.

Surface Morphology. Figure 5 shows the SEM images of the RC and the RC-*g*-PSBMA membranes after different extents of polymerization. It is obvious that the pore sizes on the membrane surfaces decreased gradually when the ATRP reaction time was prolonged, which is consistent with the DP results. After 24 h of polymerization, for example, the opening of most of the pores at the membrane surface appeared to be significantly reduced and they even looked almost being completely blocked, because of the high DP of the membrane. To achieve a good stimuli-responsive performance, the pore size of the prepared membrane surface should be comparable with the extending and/or contracting scale of the grafted polymer chains when the membrane is exposed to external stimuli. Therefore, the effective pore sizes of the prepared membranes should be controllable when fabricate stimuli-responsive membranes. The SEM images, together with the XPS analysis, suggest that the ATRP method, because of its nature of controllability in DP, can be an ideal synthesis tool for fine-tuning the effective pore sizes of the prepared membranes to achieve the desired electrolyte-responsive performance.

Electrolyte-Responsive Flux Behavior. The permeate fluxes of the RC and RC-*g*-PSBMA membranes versus the electrolyte concentrations in the solutions are shown in Figure 6. The permeate fluxes of the RC membrane exhibited an independent behaviour on the electrolyte concentrations (Figure 6a). When grafted with PSBMA, the RC-*g*-PSBMA membranes showed stimuli-sensitive permeation behaviours. For the DI water fluxes, all the different types of RC-*g*-PSBMA membranes showed increasingly smaller fluxes with the increase of the ATRP reaction times used in the membrane preparation process, in comparison with the flux of the RC membrane (see flux data at 0 M NaCl concentration in Figure 6), attributed to the additional hydraulic resistance caused by the grafted PSBMA. According to the classical Hagen−Poiseuille equation, the decreases in the fluxes may be related to the reductions in the membrane effective pore sizes (under the same operation pressure and temperature). Based on that equation (see the Supporting Information), the effective pore sizes of these membranes, corresponding to the ATRP reaction time of 6, 12, 18, and 24 h respectively, are calculated and found to be reduced to about 0.96, 0.9, 0.83, and 0.6 times of the pore size of the RC membrane.

In Figure 6b, it can be found that the permeate fluxes of the RC-*g*-PSBMA membrane that underwent 6 h of ATRP decreased gradually with the increase in NaCl concentration in the solution (at a concentration up to 0.04 M), and then the permeate flux leveled off at NaCl concentrations in the solution exceeding 0.04 M and up to 0.1 M tested. As discussed in the XPS analysis, the DP of the PSBMA chains was relatively low for only 6 h of ATRP reaction. Thus, the capability of the grafted SBMA polymers to stretch or contract with the variation of Na^+ and Cl^- ions in the solution was also low in this case. It appears that a 0.04 M NaCl solution can render all the grafted SBMA polymer chains to be fully stretched for this membrane. As a result, the flux became constant regardless of the further increase in NaCl concentration in the solution at above 0.04 M. For the RC-*g*-PSBMA membranes with longer PSBMA chains (Figure 6c,d), the fluxes decreased continuously as the concentration of NaCl in the solution increased and approached 0.1 M. Because the pore opening on the RC-*g*-PSBMA membrane that underwent 24 h of ATRP reaction [i.e., the case in Figure 6e] was essentially very small, it is found that nearly no flux was obtained at a NaCl concentration of 0.02 M or above in the solution, suggesting that all of the pores for the liquid flow had been totally blocked by the swell of the grafted SBMA polymers at the high NaCl concentrations.

The variations in the fluxes shown in Figure 6 may be explained by the conformational change of the PSBMA chains grafted on the membrane surfaces. Figure 7 depicts the various characteristic conformational states of the PSBMA chains in different environments. When in water, inter- and/or intrachain associations would take place because of the electrostatic attractions between the cations and anions, resulting in a collapsed or contract conformation of the PSBMA chains on the pore surface [Figure 7a]. Upon the addition of sodium chloride, the small Na^+ and Cl^- ions can penetrate to the collapsed PSBMA chains and disrupt the interactions of the ammonium and sulfonate groups, leading to an extended conformation of the SBMA polymer chains, which reduces the effective pore size of the membrane to flow [Figure 7b].

Flux Reversibility. To evaluate the reversible electrolyte-responsive behavior of the prepared membranes, the

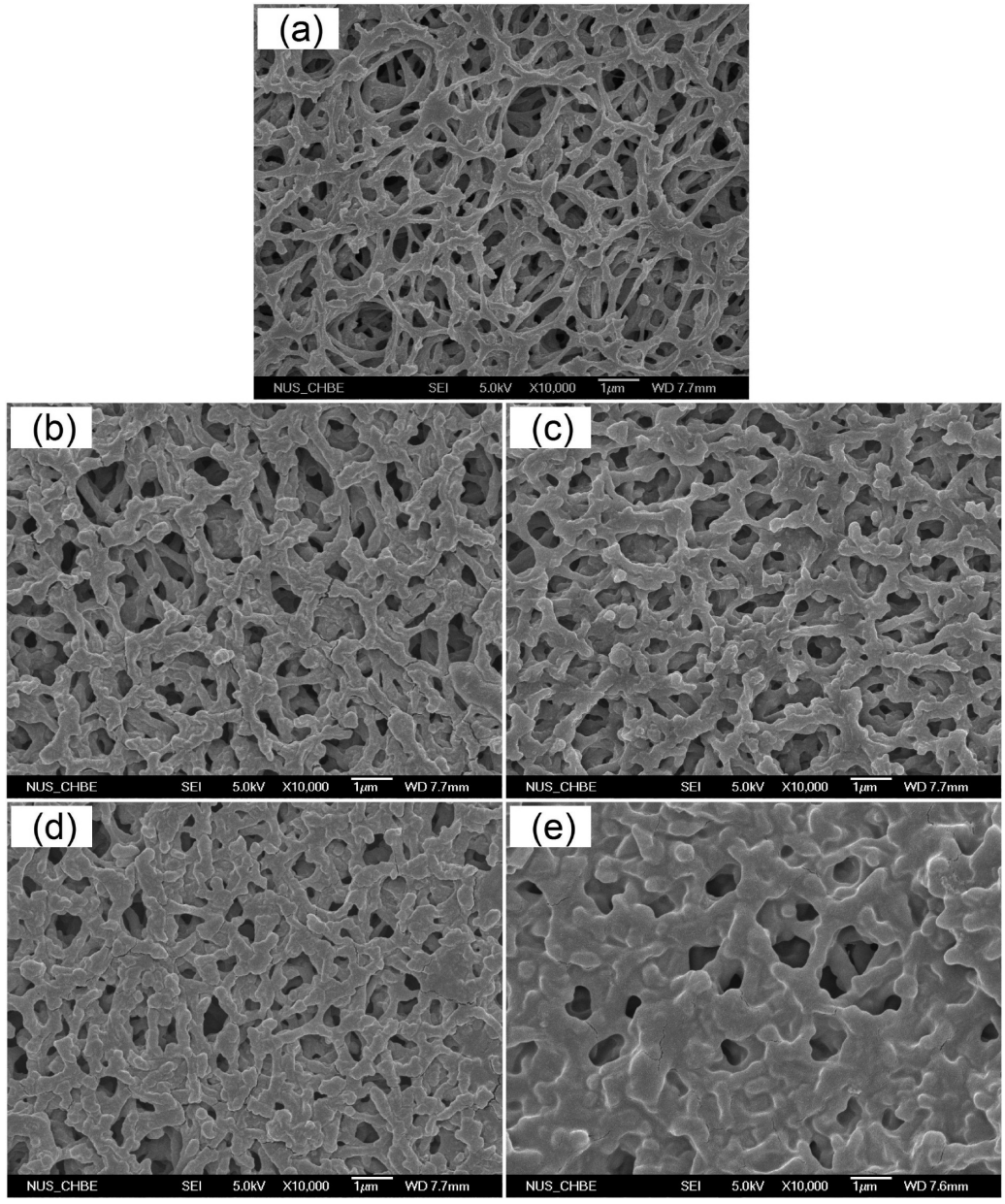

FIGURE 5. SEM surface images for (a) RC, (b−e) RC-*g*-PSBMA (ATRP conditions: [CuBr]/[$CuBr_2$]/[Bpy]/[SBMA] = 1/0.25/2/7.5; solvent, water/methanol = 1/1; ATRP reaction time (b) 6, (c) 12, (d) 18, and (e) 24 h).

RC-*g*-PSBMA membrane with 18 h of ATRP, which almost showed a switch on/off flux behavior (Figure 6d), was chosen as the sample membrane to carry out DI water and 0.1 M NaCl solution flux experiments alternately for several cycles. The fluxes of DI water or NaCl solution were measured for 1 h, respectively. After each cycle, the membrane was washed in DI water for 1 h to leach out the Na^+ and Cl^- ions captured by PSBMA. Figure 8 shows the variations of the fluxes with DI water and the 0.1 M NaCl solution. It was found that the DI water flux in the second run could not completely recover to that in the first run. After the first run, the inter- and intrachain associations of the PSBMA may be disrupted by the Na^+ and Cl^- ions and the PSBMA chains existed in an extended conformation, as discussed above (Figure 7). It may be speculated that after the Na^+ and Cl^- ions were leached out by washing, the already extended

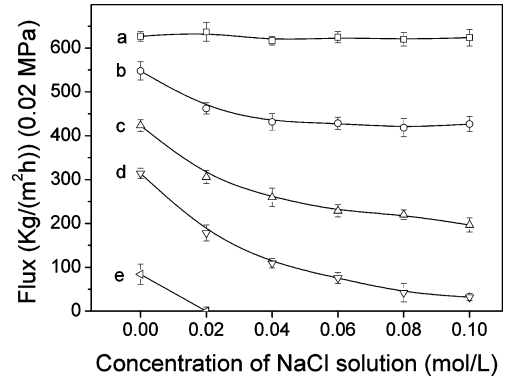

FIGURE 6. Electrolyte concentration-dependent flux of the aqueous solution through (a) RC, (b−e) RC-*g*-PSBMA (ATRP conditions: [CuBr]/[$CuBr_2$]/[Bpy]/[SBMA] = 1/0.25/2/7.5; solvent, water/methanol = 1/1; ATRP reaction time (b) 6, (c) 12, (d) 18, and (e) 24 h).

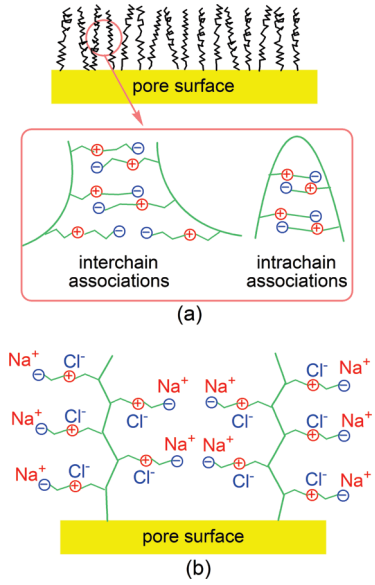

FIGURE 7. Various characteristic conformational states of PSBMA polymer chains in (a) DI water and (b) NaCl solution.

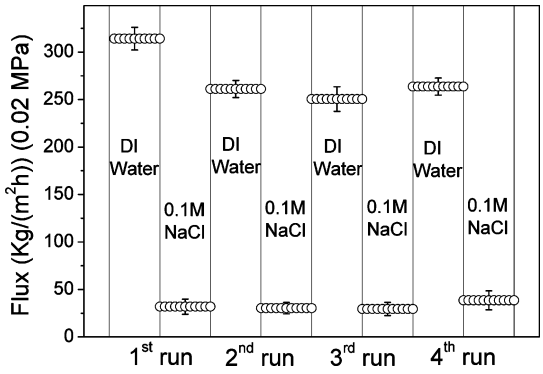

FIGURE 8. Reversible electrolyte-responsive behavior of RC-*g*-PSBMA. (ATRP conditions: [CuBr]/[$CuBr_2$]/[Bpy]/[SBMA] = 1/0.25/2/7.5; water/methanol = 1/1; ATRP reaction time = 18 h).

PSBMA chains were prone to collapse again by inter-chain associations rather than intrachain associations, because it is relatively difficult for the latter to happen because of the steric hindrance. Therefore, the effective pore size of the membrane might be somewhat smaller than that of the freshly prepared membrane, leading to a lower DI water flux (second run). This speculation is supported by the DI water fluxes that were almost completely recovered in the third and fourth runs to that of the second run, suggesting that only the disruption and formation of the inter-chain associations happened from the second run to the forth run. The results in Figure 8 indicate that the membranes prepared in this study possess a good reversible stimuli-responsive property, which is essential for practical applications.

Rejection Performances. To investigate the potential application of the prepared electrolyte-responsive membranes in protein purification, BSA solutions and polystyrene nanoparticle (NP) suspensions at different NaCl concentrations were filtered through the RC-*g*-PSBMA membrane (ATRP of 18 h). Figure 9 compares the changes in BSA and NP rejection rates induced by the concentrations of NaCl in the solutions. As expected, the BSA rejection rates were at

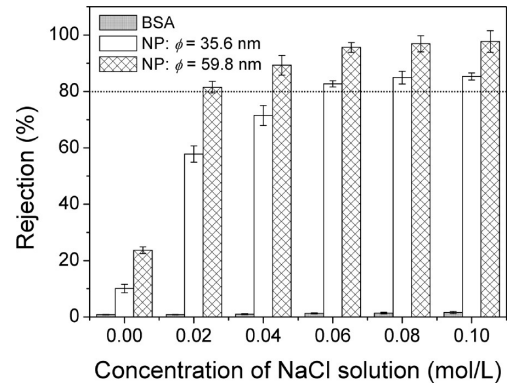

FIGURE 9. Dependence of rejection rates of BSA and NPs upon the concentration of NaCl solutions. (RC-*g*-PSBMA: [CuBr]/[$CuBr_2$]/[Bpy]/[SBMA] = 1/0.25/2/7.5; water/methanol = 1/1; ATRP reaction time = 18 h).

a very low level regardless of the concentrations of NaCl in the solutions, indicating that the membrane allowed BSA to pass through. For the NPs, the rejection rates increased remarkably with the increase of the concentrations of NaCl in the solutions. If we define the separation target of a membrane as a particle diameter cut-off (PDCO), i.e., the smallest particle diameter that has a rejection rate of 80−100%, it can be found from Figure 9 that the PDCO of the membrane reduced from around 60 nm to about 36 nm when the concentration of NaCl in the solutions increased from 0.02 to 0.06 M (see the dotted line in Figure 9). These results indicate that BSA could be efficiently separated from the different sized NPs by altering the concentration of the electrolyte. In this study, the BSA was chosen as a model protein to be purified, while the polystyrene nanoparticles represented the impurities such as virus with larger particle sizes that were to be removed. Although the pore size distribution of a membrane surface is usually too broad to achieve a discrete (or clear cut) separation performance and the rejection rate by the used membrane to the 60 nm and 36 nm NPs in this study may not be significantly different, the results shown in Figure 9 do throw a light upon the possibility of purifying one specific sized protein from impurities of different sizes using the same membrane. For example, if the size of the impurities to be separated is large, a high rejection rate can be readily achieved at a low electrolyte concentration; on the contrary, if the size is small, a high rejection rate can be realized by increasing the electrolyte concentration in the solution.

Anti-Protein-Fouling Performance. A major problem in protein filtration is the decay of membrane performance because of protein adsorption. To investigate the protein-fouling resistance of the RC-*g*-PSBMA membrane, we carried out filtration experiments with PBS and BSA solutions. Typical results for the permeation fluxes of PBS solution and BSA solution through the RC-*g*-PSBMA membrane are shown in Figure 10. It can be seen that the permeate fluxes of BSA solution declined with the filtration time, and then gradually leveled off. The decline in the permeate flux was due to the deposition or adsorption of some protein molecules on the membrane surface, which incurred the so-called membrane fouling. After the BSA

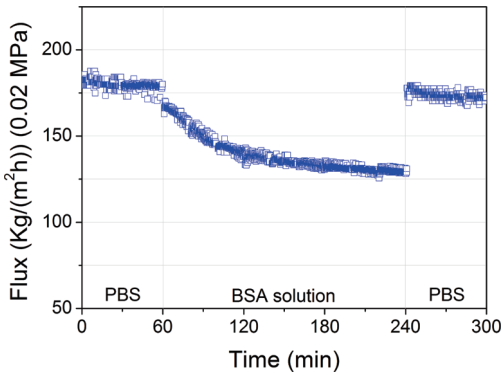

FIGURE 10. Protein-fouling behavior of the RC-*g*-PSBMA membrane. (RC-*g*-PSBMA: [CuBr]/[$CuBr_2$]/[Bpy]/[SBMA] = 1/0.25/2/7.5; water/methanol = 1/1; ATRP reaction time = 18 h).

solution filtration, the RC-*g*-PSBMA membrane was washed and then the PBS flux was measured again under the same operation conditions. It can be clearly seen in Figure 10 that the pure PBS flux almost recovered to the original level, suggesting that most of the protein-fouling for the membrane was reversible. It has been reported that the zwitterionic SBMA polymers are a kind of biocompatible material with excellent anti-protein-fouling property (34). The fundamental part of the anti-protein-fouling behavior of the zwitterionic SBMA polymers lies in their strong capacity to form a hydration layer via electrostatic interaction rather than hydrogen bond between zwitterions and water molecules, which possibly prevents protein molecules from close contact with the membrane surface to form firm bonds that contribute to irreversible fouling (47).

CONCLUSIONS

A novel electrolyte-responsive membrane was prepared by grafting zwitterionic SBMA polymers to RC membrane via surface-initiated ATRP. XPS analysis revealed that the ATRP process was affected by the concentration of the deactivator. The addition of a small amount of $CuBr_2$ could effectively reduce the polymerization rate and thus led to a more controllable polymerization process, which is of great importance for fine-tuning the pore size of the stimuli-responsive membranes to be developed. Due to the interaction of the zwitterionic SBMA polymers with the electrolyte, the flux through the RC-*g*-PSBMA membrane was found to decrease as the electrolyte concentration in the solution increased, exhibiting tunable permeation selectivity. Results showed that the electrolyte-responsive behavior of the prepared RC-*g*-PSBMA membrane was reversible. Rejection experiments with BSA and polystyrene nanoparticles demonstrated the possibility that the RC-*g*-PSBMA membrane could be used to separate proteins from impurities of different sizes through the change of electrolyte concentrations in the solution. Membranes with such properties will have a great potential for protein purification and other separation applications.

Acknowledgment. The financial support from the Ministry of Education Singapore, through R-288-000-046-112, the Academic Research Fund of National University of Singapore, is acknowledged.

Supporting Information Available: The detailed synthesis procedure of polystyrene nanoparticles, the TEM images, and size distribution of the synthesized polystyrene nanoparticles, and the method to estimate pore size with the Hagen−Poiseuille equation can be found in the Supporting Information. This material is available free of charge via the Internet at http://pubs.acs.org.

REFERENCES AND NOTES

(1) Walsh, G. *Nat. Biotechnol.* **2006**, *24*, 769–776.
(2) Feins, M.; Sirkar, K. K. *Biotechnol. Bioeng.* **2004**, *86*, 603–611.
(3) Reis, R. v.; Zydney, A. *Curr. Opin. Biotechnol.* **2001**, *12*, 208–211.
(4) Huang, R.; Kostanski, L. K.; Filipe, C. D. M.; Ghosh, R. *J. Membr. Sci.* **2009**, *336*, 42–49.
(5) Lee, D.; Nolte, A. J.; Kunz, A. L.; Rubner, M. F.; Cohen, R. E. *J. Am. Chem. Soc.* **2006**, *128*, 8521–8529.
(6) Tokarev, I.; Orlov, M.; Minko, S. *Adv. Mater.* **2006**, *18*, 2458–2460.
(7) Ulbricht, M. *Polymer* **2006**, *47*, 2217–2262.
(8) Zhang, H.; Ito, Y. *Langmuir* **2001**, *17*, 8336–8340.
(9) Ito, Y.; Park, Y. S.; Imanishi, Y. *J. Am. Chem. Soc.* **1997**, *119*, 2739–2740.
(10) Ito, Y.; Ochiai, Y.; Park, Y. S.; Imanishi, Y. *J. Am. Chem. Soc.* **1997**, *119*, 1619–1623.
(11) Bai, D.; Elliott, S. M.; Jennings, G. K. *Chem. Mater.* **2006**, *18*, 5167–5169.
(12) Friebe, A.; Ulbricht, M. *Macromolecules* **2009**, *42*, 1838–1848.
(13) Jin, X.; Hsieh, Y.-L. *Polymer* **2005**, *46*, 5149–5160.
(14) Schacher, F.; Rudolph, T.; Wieberger, F.; Ulbricht, M.; Müller, A. H. E. *ACS Appl. Mater. Interfaces* **2009**, *1*, 1492–1503.
(15) Schacher, F.; Ulbricht, M.; Müller, A. H. E. *Adv. Funct. Mater.* **2009**, *19*, 1–6.
(16) Li, Y.; Chu, L.-Y.; Zhu, J.-H.; Wang, H.-D.; Xia, S.-L.; Chen, W.-M. *Ind. Eng. Chem. Res.* **2004**, *43*, 2643–2649.
(17) Park, Y. S.; Ito, Y.; Imanishi, Y. *Langmuir* **1998**, *14*, 910–914.
(18) Chu, L.-Y.; Li, Y.; Zhu, J.-H.; Chen, W.-M. *Angew. Chem. Int. Ed.* **2005**, *44*, 2124–2127.
(19) Yang, W.-C.; Xie, R.; Pang, X.-Q.; Ju, X.-J.; Chu, L.-Y. *J. Membr. Sci.* **2008**, *321*, 324–330.
(20) Geismann, C.; Yaroshchuk, A.; Ulbricht, M. *Langmuir* **2007**, *23*, 76–83.
(21) Guilherme, M. R.; Moura, M. R. d.; Radovanovic, E.; Geuskens, G.; Rubira, A. F.; Muniz, E. C. *Polymer* **2005**, *46*, 2668–2674.
(22) Lequieu, W.; Prez, F. E. D. *Polymer* **2004**, *45*, 749–757.
(23) Kang, M.-S.; Martin, C. R. *Langmuir* **2001**, *17*, 2753–2759.
(24) Lee, S. B.; Martin, C. R. *J. Am. Chem. Soc.* **2002**, *124*, 11850–11851.
(25) Mika, A. M.; Childs, R. F.; Dickson, J. M.; McCarry, B. E.; Gagnon, D. R. *J. Membr. Sci.* **1995**, *108*, 37–56.
(26) Phillips, A. K.; Moore, R. B. *Polymer* **2005**, *46*, 7788–7802.
(27) Chung, D.-J.; Ito, Y.; Imanishi, Y. *J. Appl. Polym. Sci.* **1994**, *51*, 2027–2033.
(28) Lowe, A. B.; McCormick, C. L. *Chem. Rev.* **2002**, *102*, 4177–4190.
(29) Schulz, D. N.; Peiffer, D. G.; Agarwal, P. K.; Larabee, J.; Kaladas, J. J.; Soni, L.; Handwerker, B.; Garner, R. T. *Polymer* **1986**, *27*, 1734–1742.
(30) Liaw, D.-J.; Huang, C.-C. *Macromol. Symp.* **2002**, *179*, 209–222.
(31) Chen, L.; Honma, Y.; Mizutani, T.; Liaw, D.-J.; Gong, J. P.; Osada, Y. *Polymer* **2000**, *41*, 141–147.
(32) Kudaibergenov, S. E.; Sigitov, V. B. *Langmuir* **1999**, *15*, 4230–4235.
(33) Mary, P.; Bendejacq, D. D.; Labeau, M.-P.; Dupuis, P. *J. Phys. Chem. B* **2007**, *111*, 7767–7777.
(34) Zhang, Z.; Chen, S.; Chang, Y.; Jiang, S. *J. Phys. Chem. B* **2006**, *110*, 10799–10804.
(35) Zhang, Z.; Chao, T.; Jiang, S. *J. Phys. Chem. B* **2008**, *112*, 5327–5332.
(36) Li, G.; Xue, H.; Cheng, G.; Chen, S.; Zhang, F.; Jiang, S. *J. Phys. Chem. B* **2008**, *112*, 15269–15274.
(37) Bhut, B. V.; Wickramasinghe, S. R.; Husson, S. M. *J. Membr. Sci.* **2008**, *325*, 176–183.
(38) Singh, N.; Chen, Z.; Tomer, N.; Wickramasinghe, S. R.; Soice, N.; Husson, S. M. *J. Membr. Sci.* **2008**, *311*, 225–234.

(39) Singh, N.; Wang, J.; Ulbricht, M.; Wickramasinghe, S. R.; Husson, S. M. *J. Membr. Sci.* **2008**, *309*, 64–72.
(40) Bhut, B. V.; Husson, S. M. *J. Membr. Sci.* **2009**, *337*, 215–223.
(41) Lovell, P. A.; El-Aasser, M. S. *Emulsion Polymerization and Emulsion Polymers*; Wiley: New York, 1997.
(42) Patten, T. E.; Matyjaszewski, K. *Adv. Mater.* **1998**, *10*, 901–915.
(43) Matyjaszewski, K.; Miller, P. J.; Shukla, N.; Immaraporn, B.; Gelman, A.; Luokala, B. B.; Siclovan, T. M.; Kickelbick, G.; Vallant, T.; Hoffmann, H.; Pakula, T. *Macromolecules* **1999**, *32*, 8716–8724.
(44) Iwata, R.; Suk-In, P.; Hoven, V. P.; Takahara, A.; Akiyoshi, K.; Iwasaki, Y. *Biomacromolecules* **2004**, *5*, 2308–2314.
(45) Husseman, M.; Malmström, E. E.; McNamara, M.; Mate, M.; Mecerreyes, D.; Benoit, D. G.; Hedrick, J. L.; Mansky, P.; Huang, E.; Russell, T. P.; Hawker, C. J. *Macromolecules* **1999**, *32*, 1424–1431.
(46) Matyjaszewski, K.; Xia, J. *Chem. Rev.* **2001**, *101*, 2921–2990.
(47) Ishihara, K.; Nomura, H.; Mihara, T.; Kurita, K.; Iwasaki, Y.; Nakabayashi, N. *J. Biomed. Mater. Res.* **1998**, *39*, 323–330.

AM900654D